Polymer Journal (2014) 46, 469–475

www.nature.com/pj

FOCUS REVIEW

Development of functional polyplex micelles for systemic gene therapy

Kensuke Osada[1,2]

Recent advances in chemistry-based engineering have developed smart nanodevices for realizing targeted therapy by rationally integrating versatile molecular technologies to achieve specific structures and functionalities. Gene therapy is one of the most intriguing targets, because nanodevices to deliver fragile DNA into pathological cells and exert effective transgene expression are indispensable for achieving this innovative therapeutic modality. The largest challenge lies in the development of an appropriate systemic delivery system that can withstand the harsh environment of circulating blood and efficiently accumulate in a targeted location for gene expression. This review focuses mainly on our polymer-based DNA delivery systems, which are fabricated from polyion complexation between plasmid DNA and functionalized poly(ethylene glycol)-based block catiomers, and highlights their development to systemic settings for application to cancer treatment.
Polymer Journal (2014) **46,** 469–475; doi:10.1038/pj.2014.49; published online 18 June 2014

GENE DELIVERY SYSTEMS FOR SYSTEMIC APPLICATIONS

Significant advances in chemistry-based engineering have promoted the development of a variety of smart nanodevices, which brought about breakthroughs in medical care.[1–5] Gene delivery systems are a fascinating example because smart nanodevices that encapsulate and deliver a therapeutic gene to a pathological site, followed by functional protein expression, are inevitable to establish this therapeutic modality. The concept of gene therapy, when first conceived, was accompanied by substantial expectations for treating a broad variety of intractable diseases.[6] Nevertheless, its clinical application has long been hampered because of the lack of sufficient methodology to demonstrate efficient gene transfer, particularly after systemic administration. The systemic administration was particularly anticipated because of the tremendous advantage in accessibility to target sites via the circulatory system, thereby allowing multiple treatments without surgery.

Viruses was considered as attractive delivery system because of their inherent abilities as natural gene delivery systems, and some of these were developed to clinical stages (http://www.abedia.com/wiley/countries.php).[7] However, most of their systemic applications have been limited because of elimination by host immune defenses. Moreover, viral vectors also have several critical drawbacks, including intrinsic immunogenicity, limited gene size loading and difficulty of large-scale production. Therefore, development of systemically applicable non-viral DNA delivery systems is highly expected to establish this potent therapeutic modality.

Toward this aim, a vast amount of research has attempted to fabricate gene delivery carriers. However, systemic application remains challenging,[8] although certain therapeutic effects have been achieved by local application, that is, direct injection into pathological sites. The primary problem that hinders systemic applications is inadequate retention in circulation. A number of inherent biological barriers undermine their retention in the bloodstream, including nuclease digestion, harsh physiological environments and capture by the macrophages of the mononuclear phagocytic system (MPS).[9] Apart from circulatory retention, selective accumulation to target sites and conducting efficient gene expression are also critical for developing efficient systemic applications. To overcome these issues, gene delivery systems must be strategically fabricated into appropriate structures and armed with desirable functionalities.

POLYPLEX MICELLES (PMs) AS POTENTIAL CARRIERS FOR SYSTEMIC DELIVERY

Pursuing systemic delivery, our group pioneered polymeric micelles designated as PMs as potent gene carriers fabricated via an electrostatic interaction-mediated self-assembly process of block copolymers of poly(ethylene glycol) (PEG)-polycations and plasmid DNA (pDNA).[10] The PMs have a characteristic core-shell architecture in which pDNA is packaged into a core compartment as a consequence of DNA condensation triggered by complexation with a polycation segment, whereas PEG chains are tethered to the complex core as a shell compartment. It is important to note that the PEG compartment has a crucial role as a protective palisade, inhibiting nonspecific interactions with biological components and biological structures and conferring stealth property within biological environment. Indeed, the advantageous structure of PMs provides for appreciable colloidal stabilities within a biological milieu, thereby leading to therapeutic effects when used for local applications.[11,12] However, further applications directed toward a more severe biological environment, that is, systemic administration, were still restricted despite the fact

[1]Department of Bioengineering, Graduate School of Engineering, University of Tokyo, Tokyo, Japan and [2]Japan Science and Technology Agency, PRESTO, Saitama, Japan
Correspondence: Professor K Osada, Department of Bioengineering, Graduate School of Engineering, University of Tokyo, 7-3-1 Hongo, Tokyo 113-8656, Japan.
E-mail: osada@bmw.t.u-tokyo.ac.jp
Received 12 March 2014; revised 24 April 2014; accepted 24 April 2014; published online 18 June 2014

that the advantageous structure of PMs indeed improved survival in the circulatory system.[13] Further enhancement of the structural stability and stealth property of PMs was still required for systemic applications.

To this end, we revisited to investigate structure of PMs with a prospect that such essential knowledge would propose rational material design concepts to advance PMs for systemic setting. The initial studies focused on the precise determination of PM structure, especially how pDNA was packaged within the core and how many PEG chains were tethered to it as a shell. These studies led to the identification of factors that govern both packaging structure of pDNA in the core and PEG crowdedness. Then, we developed PMs to enhance PEG shielding and reinforce structural stability based on the fundamental understanding leaned from these structural studies. Ultimately, pilot molecules targeting a specific site were installed on these strengthened PMs to achieve targeted systemic gene delivery.

In this review, two basic PMs fabricated from PEG-poly(L-lysine) (PEG-PLys)[10] and PEG-poly{*N*′-[*N*-(2-aminoethyl)-2-aminoethyl] aspartamide} [PAsp(DET)] (PEG-PAsp(DET)) block copolymers[14] are focused among the variety of functional block copolymers developed to date.[15] PEG-PLys having polymerized cationic amino-acid L-lysine was used for basic studies to acquire insights into PM structures. The PEG-PAsp(DET), which was obtained from a screening study to find appropriate cationic species by the aminolysis technique,[14] was used to promote biological functions because of its fascinating characteristics, such as pH-responsive endosome disruption[16] and self-degradability after incubation at physiological temperatures, which reduce the cumulative toxicity.[17]

pDNA PACKAGING WITHIN PMs AND DETERMINING THE REGULATING FACTORS INVOLVED

Quantized folding of pDNA to form a core compartment

PEGylated gene carriers commonly form particles of approximately 100 nm through DNA condensation,[18] which is a valid size to expect tumor accumulation through the enhanced permeability and retention effect.[19] However, a precise structure for pDNA packaging within the particle had been under the veil. To advance the PMs toward systemic setting, unveiling of this issue should endow a solid base in designing to desired formulation. When considering that pDNA is a rigid and long macromolecule (micrometer-length) with supercoiled closed circular form, pDNA packaging into 100 nm-sized particles seems quite mysterious. Thus, we concentrated our efforts on clarifying the detailed structure of pDNA packaged within PMs. Transmission electron microscopy observations revealed that pDNA was packaged into rod-like shapes with several 100 nm in length to form a core compartment (Figure 1). This suggested that pDNA had folded several times to finally settle as a bundle in the core. In this scheme, DNA at the rod end had to be sharply folded; however, this was not acceptable in that view of rigid double-stranded DNA exhibiting a persistence length (l_p) of 50 nm.[20] We approached this issue with regard of the inherent rigidity of double-stranded DNA and the topological restrictions of its supercoiled form. Finally, a highly ordered folding scheme for pDNA was proposed with an intriguing trick. pDNA was folded into rod-like structures with a regulated rod length, as quantized lengths of $1/(2n+1)$ multiples of the original pDNA contour length by n times folding.[21] The sharp folding occurred by local dissociation of the characteristic double-stranded structure at each folding site,[22] that is, rod end. It is noteworthy that DNA rigidity originates from the helical structure of its double-stranded form, thus the single-stranded DNA is a flexible chain with an l_p of only a few nanometers[23] or less.[24] In this way, the precise scheme of packaging pDNA into the rod or filament shapes, which are often observed in various PM systems, was unveiled.[25–27]

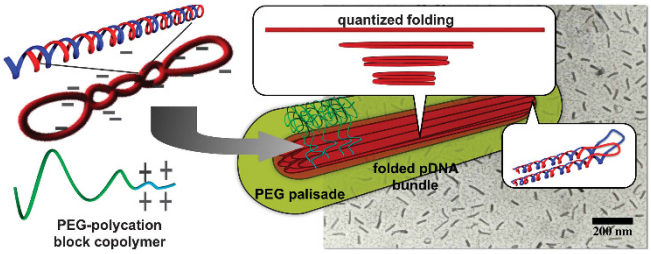

Figure 1 Plasmid DNA (pDNA) packaging in polyplex micelles through polyion complexation with poly(ethylene glycol) (PEG)-polycation block copolymers. A pDNA is packaged into rod-shaped core as shown on transmission electron microscope imaging by obeying a regulated folding scheme, 'quantized folding' and the core is surrounded by a PEG shell. DNA at the rod end is folded concomitant with local double-strand dissociation.

Regulating factors determining rod length in PMs

Interestingly, the length of a folded rod was significantly affected by the cationic segment length (degree of polymerization, DP) of block copolymers. PMs prepared from PEG-PLys block copolymers with a fixed PEG molecular weight (M_w) of 12 kDa and varying PLys DP (19–70) exhibited changes in their rod lengths; shorter with increasing PLys DP and longer with decreasing PLys DP.[28] These findings suggested that PLys DP could control rod length, in other word, the folding number. Notably, the distributions of rod lengths with different PLys DP consistently adhering to the quantized folding scheme, validating the folding scheme.

To gain insights on the underlying principles involved in the regulation of rod length by PLys DP, an analysis of energetic contributions to PMs was made. Because a PM is essentially formed by charge neutralization between pDNA and PEG-PLys block copolymers, a change of PLys DP indicates a simultaneous change in the binding polymer number to pDNA. This, in turn, indicates that the number of PEG chains tethered to a pDNA molecule is a function of PLys DP. Therefore, the pDNA packaging structure was elucidated from the standpoint of PEG. To assess this quantitatively, the extent of PEG crowdedness must be known. However, to the best of our knowledge, it has not been accurately quantified for any type of PEGylated gene delivery system, despite the widespread use of PEGylation. This is because the two requirements for calculating PEG density were missing: the surface area of the core to which the PEG chains are tethered and the number of PEG chains tethered there. Regarding this point, our finding of the quantized folding scheme of pDNA provided the necessary geometrical information to calculate the core surface area. Moreover, we established a method to determine the number of PEG chains tethered to a single pDNA using ultracentrifuge analysis[29] and thereby fulfilled the requirements to calculate the PEG density. These findings allowed identification of PEG crowdedness in PMs for the first time. Consequently, PEG crowdedness was found to increase with decreasing PLys DP (Figure 2a) with a suggestion that the PEG conformation changed from an overlapping mushroom conformation (for PLys DP 69) to an upward squeezing conformation (for PLys DP 39 and 19).[30] This observation was actually supported by cryogenic transmission electron microscope observations (Figure 2b), which provided direct measurements of PEG height, $<H>$, by dividing the width of a parallel adjacent rod by 2 (Figure 2a). Based on this observation,

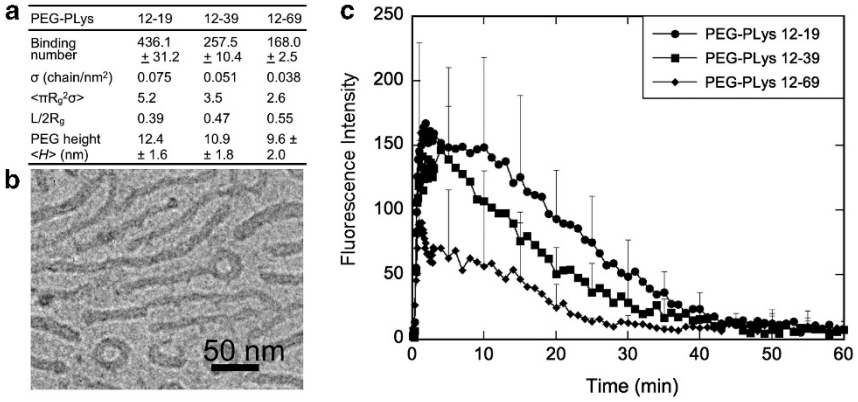

Figure 2 Poly(ethylene glycol) (PEG) crowdedness and blood circulation profiles of polyplex micelles (PMs) prepared from PEG-PLys. (**a**) Summarized data for PEG crowdedness. (**b**) Representative cryogenic transmission electron microscope image at a locally concentrated region of PMs with PLys39, from which the average PEG height, $<H>$, was estimated. (**c**) Blood circulation profiles for PMs prepared with different poly(L-lysine) degree of polymerization and Cy5-labeled pDNA observed in *in vivo* real-time confocal laser scanning microscope (CLSM) on the ears of mice (All three curves have *P*-values <0.05 by analysis of variance.). Standard errors of the mean (s.e.m.) are shown at representative times. Figures modified from Tockary *et al.*[30]

$<H>$ for PMs of PLys 69 was determined to be 9.6 nm, which corresponded well with the theoretical H of a mushroom conformation (9.4 nm: $2R_g$ of PEG with $M_n = 12$ K), whereas those for PLys 39 and 19 were higher (Figure 2a). These observations affirmed the reasonability of the PEG conformation suggested above.

Subsequent analysis of rod lengths in terms of energetic contributions led to the proposition that pDNA packaged within PMs is regulated by an interplay of the following compaction and anti-compaction forces. The unfavorable surface energy developed at the interface of a pDNA/PLys complex core and water molecules emerges the compaction force to reduce the surface area. On the other hand, the PEG steric repulsion, which comprises osmotic pressure from crowded PEG and entropic elasticity originating from the restricted conformation, and the rigidity of folded DNA as a bundle contribute as anti-compaction force.[30] This analysis intuitively describes higher PEG crowdedness and longer rod length for PMs of lower PLys DP. A larger number of PEG chains are tethered on the packaged pDNA core prepared from lower PLys DP because a larger number of PEG-PLys block copolymers are required to neutralize the negative charges of pDNA. In contrast, PEG chains do not like a densely packed situation; thus, they tend to extend the area of the PEG tethering site (core) to acquire more space for chains to take an expanded conformation, eventually leading to longer rods. Although the longer rod cost more unfavorable surface energy, this was counterbalanced by an increased repulsive force from more crowded PEG. Accordingly, this interpretation reasonably accounts for the structural observations of PMs at different PLys DP and also provides a principle for controlling PM structure for the desired form directed toward systemic delivery use.

PMs FOR PROLONGED BLOOD CIRCULATION TIME

PMs must circumvent numerous biological obstacles to circulate in the bloodstream in an intact form. The primary obstacle is their recognition by macrophages of the MPS, which is triggered by the adsorption of opsonin proteins presented in the blood.[9] In addition, interactions with polyanionic species during circulation are major obstacles because these can trigger polyion exchange reactions, which result in the disintegration of electrostatically assembled PMs. Furthermore, nuclease digestion accelerates the destabilization of these assemblies, although PMs certainly provide a certain level of resistance against nucleases.[10] To overcome these obstacles, improvements were made to both the PEG and the core compartments of PMs.

Modifications of PEG compartments for improved blood circulation properties

The analysis of PEG crowdedness on the PMs provided an opportunity to clarify the correlation between actual PEG crowdedness of the PMs and blood circulation profiles, which had not been clarified despite the importance of PEGylation.[31–33] It should be noted that a study of inhibition of serum protein adsorption onto a PEG modified surface indicated that PEG in a squeezed conformation could efficiently inhibit serum protein adsorption, whereas that PEG in a mushroom conformation was still prone to adsorption.[34] Therefore, prolonged blood circulation was expected for PMs that were obtained from lower PLys DP as they exhibited more PEG crowding. Subsequent evaluations of blood retention showed good agreement with this expectation (Figure 2c). Noteworthy, at the initial period, a certain amount of PMs appeared after injection of PLys 19 and 39, whereas this was limited for PLys 69, which suggested the relevance of PEG crowdedness to the circulation profile. It is likely that PEG in a mushroom conformation (PLys 69) was still subject to serum protein adsorption and thus was more susceptible to MPS capture and subsequently elimination after the injection. This result presented an important message that regulating PEG crowdedness into a squeezed or possibly more crowded brush region was essential for PMs to ensure a prolonged circulation property.

Reinforcing core compartments to improve blood circulation properties

Along with enhancing PEG shielding, reinforcing structural stability to prevent polyion exchange-mediated disassembly also proved to be an effective strategy in prolonging circulation in the blood. We demonstrated two strategies, namely core cross-linking and the use of hydrophobic moieties to add a coagulation force.

Cross-linking via disulfide bonds is an attractive strategy because not only do these cross-links stabilize the assembly but they are reversibly cleaved in the intracellular reductive environment in response to a higher glutathione concentration (~ 10 mM)[35] compared with that of the extracellular environment ($\sim 10\,\mu$M). This cleavage triggers the liberation of encapsulated pDNA for transcription.[36] Indeed, cross-linked PMs (CPMs) prepared from

PEG-PLys with a flanking SH group in its side chain exhibited remarkable tolerance against polyelectrolyte exchange reactions,[36] which established cross-linking as a valid strategy to avoid disassembly in the presence of polyanions. Consequently, increased blood retention was obtained for CPMs.[37] It is worth noting that these CPMs remarkably promoted transfection efficiency, which simultaneously verified the cleavage of disulfide cross-links in response to the intracellular environment.

Introducing a hydrophobic molecule into core-forming segment of the block copolymer is also attractive because it could increase the coagulation force and prevent dissociation. In addition, it could also facilitate more polymers binding to pDNA by exceeding the charge stoichiometric ratio. Importantly, an energetic analysis of PMs predicted that an increased coagulation force drives a core to be more compact. Accordingly, it is expected that an increased number of tethering PEG chains would settle onto a more compact core, thus synergistically increasing PEG crowdedness, by prevailing the steric repulsion. To this end, a hydrophobic cholesteryl group was introduced at the ω-terminus of a PEG-PAsp(DET) block copolymer with PEG M_w of 12 kDa (PEG12C).[38] Quantification of the binding number of block copolymers to pDNA showed an increased binding number in response to an increase in the fed block copolymers. In contrast, the binding number remained constant for non-cholesteryl PEG-PAsp(DET) block copolymers (PEG12), which maintained charge stoichiometric complex formation.[29] Moreover, the rod length was found to be shorter for PEG12C PMs compared with PEG12 PMs, which confirmed the expectation of more PEG tethering on a smaller core, leading to elevated PEG crowdedness.[38] Increasing the PEG M_w to 20 kDa (PEG20C) further increased PEG crowdedness. Ultimately, an analytical investigation of PEG crowdedness suggested the possibility that the PEG conformation was reaching a scalable brush conformation.[38] The enhanced PEG shielding may also contribute to preventing nucleases and polyanions from accessing the core compartment. Indeed, PMs of PEG20C exhibited remarkable tolerance against attack by nucleases and polyanions compared with that of PEG12C and PEG12. Consequently, the conjugation of cholesteryl groups improved blood circulation profiles (PEG12 vs PEG12C), and the increased PEG M_w further improved the profiles (PEG12C vs PEG20C; Figure 3a), which validated the strategic use of hydrophobic molecules to improve blood retention time. It is interesting to note that the circulation profiles suggested that PMs of PEG20C might have completely escaped the early elimination event, as extrapolation of the retention profiles to time 0 showed 100% of the initial dosage used.[38]

LIGANDS TO RESOLVE THE PEG DILEMMA OF STEALTH VS CELLULAR UPTAKE

Increased PEG shielding is necessary to prolong blood circulation, as shown above. At the same time, this effort results in a trade-off of transfection efficiency, as high PEG shielding reduces PM affinity to cell membranes and hinders cellular uptake, known as the PEG dilemma. To overcome this dilemma, two main strategies have been addressed. One is site-specific PEG cleavage to enhance cell membrane affinity.[39–42] The other is modifying the particle surface with specific ligands such as antibodies,[43] cell membrane penetration peptides[44–46] or peptides that recognize specific receptors that are highly expressed on the membranes of target cells.[47–50]

The PEG dilemma was indeed elicited in the longer PEG chains of PMs, PEG20C ($M_w = 20$ k), which exhibited reduced uptake compared with PMs of PEG12C ($M_w = 12$ k).[38] Therefore, we modified PMs with peptides to improve cellular uptake. Here, cyclic RGD (Arg-Gly-Asp) (cRGD) peptides,[51] which recognize $\alpha_v\beta_3$ and $\alpha_v\beta_5$ integrins overexpressed on tumor cells and tumor neovascular endothelial cells, were chosen as ligands and used to prepare cRGD-installed PMs (R-PMs). Of note, the cRGD peptides concomitantly afford tumor targeting after systemic administration. Installation of cRGD actually managed to overcome the PEGylation hindrance of cellular uptake as evidenced by a remarkable increase of *in vitro* uptake efficiency of R-PEG20C compared with the limited uptake level of PEG20C in cells that overexpressed these integrins. Notably, this cRGD effect was particularly pronounced when applied to highly PEG shielded PMs. Cellular uptake investigated by confocal laser scanning microscopy showed that R-CPMs with increased PEG shielding (17 kDa PEG) exhibited a more pronounced cRGD effect than those with less (12 kDa PEG),[52] which verified the importance of high PEG shielding to elicit cRGD-mediated uptake. Concomitantly, this result suggested that the significance of using ligands for specific targeting was limited if applied to PMs with surfaces of inferior stealth.

Interestingly, confocal laser scanning microscopy studies suggested another advantage of cRGD ligands in post-endocytosis processes. R-PMs exhibited rapid migration to an area close to a cell nucleus, which was in contrast to the behavior of non-cRGD PMs.[52] This observation suggested that R-PMs adopted an alternative intracellular trafficking pathway, bypassing entrapment in digestive endosome/lysosome compartments. Ultimately, R-PMs exhibited dramatically increased transfection efficiency.[37,38] These results, when taken together, validate the utility of cRGD as a potent strategy not only for reversing the reduced cellular uptake because of increased PEG shielding but also for inducing enhanced transfection presumably owing to an alternate intracellular pathway. Importantly, this cRGD effect was particularly pronounced when applied to PMs well shielded with PEG.

SYSTEMIC TREATMENT FOR INTRACTABLE PANCREATIC CANCER

Having obtained PMs that held promise for systemic applications, their potency was then examined in systemic treatments of subcutaneous xenograft models of cancer in mice. For this purpose, pancreatic adenocarcinoma was selected as the target cancer because it is one of the most intractable solid tumors.[53] Thus, successfully treating this disease would confirm the tremendous impact of systemic gene therapy. It is notable that endothelial cells in tumor blood vessels, pericytes, fibroblasts in tumor stroma and tumor cells all overexpress $\alpha_v\beta_3$ and $\alpha_v\beta_5$ integrins, which recognize cRGD peptides. Thus, all of these cells are targeted by cRGD PMs. Furthermore, it should be noted that pancreatic tumors have poor vascular density; that is hypovascularity, in contrast to hypervascular tumors. Moreover, tumor vasculatures are covered by abundant pericytes, and tumor nests are separated by a stroma that is filled with thick fibrosis. These histological features hinder the access of PMs from the vasculature into these tumor nests. Notably, nanoparticles >50 nm in diameter are restricted in their ability to reach tumor nests.[54] In this regard, delivery of 100 nm-sized PMs as measured by dynamic light scattering into tumor nests is unlikely. Based on this histology, we targeted cells located between the vasculature and tumor nests by cRGD, with antiangiogenic approach[55,56] by transducing secreted proteins to terminate neovascularization signals and suppress tumor growth. To this attempt, we selected the soluble sFlt-1,[57] which is a receptor of

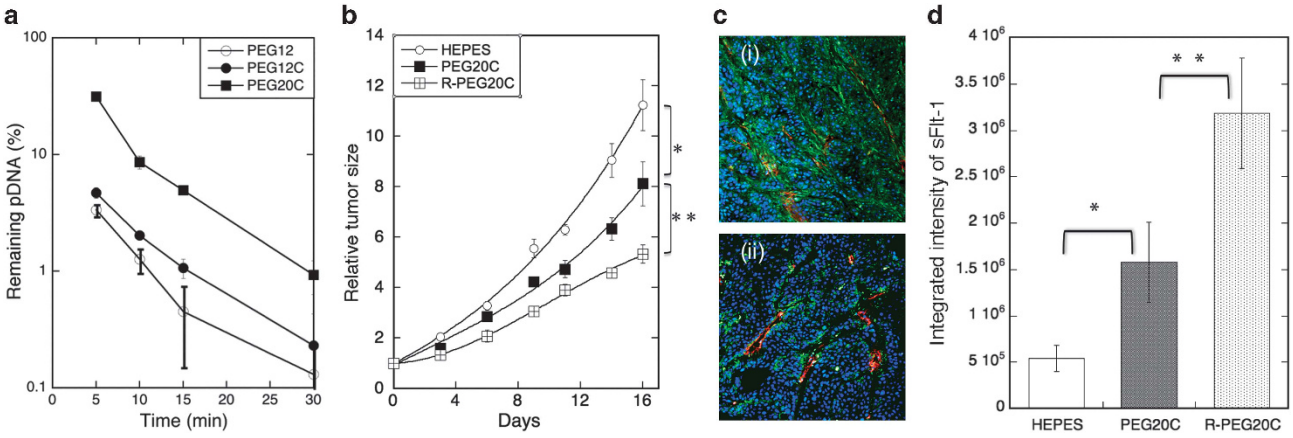

Figure 3 *In vivo* evaluations after systemic administration of PEG-PAsp(DET)-based polyplex micelles (PMs). (**a**) Promotion of blood circulation retention by cholesteryl conjugation and increased poly(ethylene glycol) (PEG) molecular weight. The remaining pDNA dose was determined by reverse transcription PCR (RT–PCR) for the collected blood samples at each time point (see Ge *et al.*[38] for details). The 100% dose was determined by subsequent measurement for the samples mixing the PMs with collected blood from a mouse. (**b**) Antitumor activity in terms of tumor size (mean ± s.e.m., $n=3$, $^{*}P<0.05$ and $^{**}P<0.01$; Student's *t*-test). (**c**) Representative immunostained confocal laser scanning microscope (CLSM) images of sFlt-1 protein expression in tumor tissues after systemic injection of cyclic RGD (Arg-Gly-Asp) (R)-PMs. (**i**) R-PEG20C, (**ii**) HEPES buffer used as a control. Green: sFlt-1; blue: nuclei; red: vascular endothelial cells. (**d**) Integrated intensities of Flt-1/VEGFR1-positive regions (green) were quantified from these images (mean ± s.e.m., $n=4$; $^{*}P<0.05$ and $^{**}P<0.01$, Student's *t*-test). Figures modified from Ge *et al.*[38]

angiogenic molecules (vascular endothelial growth factor) as a pDNA payload for treatment.

With this strategy, R-PMs stabilized by disulfide core cross-linking (R-CPMs) were injected into mice tail veins. These R-CPMs indeed induced remarkably higher sFlt-1 expression in tumor tissues as detected by Enzyme-Linked ImmunoSorbent Assay (ELISA) than those of mice injected with non-targeted PMs.[58] As a result, R-CPMs exhibited a significant tumor suppression effect. Moreover, cRGD installed to more PEG-shielded PMs (R-PEG20C) resulted potent tumor growth suppression compared with those without cRGD (Figure 3b).[38] Immunostained images of fixed cryosections of tumor tissues treated by R-PEG20C showed significantly more sFlt-1 gene expression in stromal regions than sections from non-cRGD PEG20C and control groups (Figures 3c and d). In addition, the density of vascular endothelial cells was significantly reduced in tumors treated with R-PEG20C compared with PEG20C and control groups. These results overall confirmed the effects of cRGD on well-shielded PMs for systemic targeting and facilitating antiangiogenic gene expression at the targeted tumor site, which led an antiangiogenic effect, inhibiting neovascularization and ultimately causing tumor growth suppression.

SUMMARY

Longevity in circulating blood and the ability to target tumors were required characteristics for PMs in systemic applications. Core stability was reinforced by several approaches, namely disulfide cross-linking and inclusion of hydrophobic moieties, both of which appreciably improved stability and prolonged blood circulation time. Increased circulation longevity was also achieved by increasing PEG crowdedness, which was simply obtained by using block copolymers with shorter polycations. However, this approach was not so efficient in increasing PEG crowdedness because increasing the number of tethered PEG chains resulted in longer rods, which then extended the available space for PEG tethering. Energetic analysis of rod-shaped PMs argued for the strategic use of hydrophobic molecules in block copolymers to address this issue. Cholesteryl conjugation increased binding polymer numbers with a concomitant reduction in rod length, synergistically increasing PEG crowdedness. In these ways, PEG crowdedness was substantially increased, possibly reaching scalable brush conformations, leading to increased time in blood circulation.

Tumor targeting, the second task required for systemic applications, was successfully demonstrated by installing tumor-homing molecules. This ligand effect was particularly pronounced in PMs well shielded by PEG. Ultimately, these more mature PMs exhibited significant antitumor efficacy in systemic treatment.

It should be noted that despite these extensive efforts, blood retention times did not exceed >60 min, which is in sharp contrast to stealthier nanoparticles, such as dichloro(1,2-diaminocyclohexane)-platinum(II) (DACHPt)-loaded polymeric micelles[59] or polymeric vesicles,[60] for which more than 10% of the initial dose used was still circulating even after 24 h. It is notable that estimations of PEG crowdedness in these stealthy nanoparticles identified a transition from a mushroom conformation to a squeezed conformation, which implies that this crowdedness may be sufficient to avoid initial MPS capture. Accordingly, this result suggests that PMs in our studies were eliminated by other modes because the developed PMs in our studies retained higher PEG crowdedness than the aforementioned stealthier nanoparticles. It is possible, then, that the assembly mechanism of PMs may account for this inferior blood circulation profile. PMs formed by electrostatic interactions are susceptible to dissociation by polyanions, which is most likely to occur in the glomerular basement membrane of the kidney in which heparan sulfate, a strong polyanion, is abundant.[61,62] Notably, PMs have been shown to be sufficiently stable when incubated with serum, and CPMs are demonstrated to be fairly tolerant when incubated with polyanions. This may suggest a difference in the effects of static incubation on PMs and dynamic flow in blood circulation. Possibly, the substantial shear stress of systemic conditions may increase the susceptibility of PMs to dissociate during interactions with heparan sulfate in the glomerular basement membrane. PMs under these conditions may eventually lose their resistance to nuclease attack and ultimately be captured by the MPS. When taken together, these obstacles could be responsible for the elimination of PMs from bloodstream.

Finally, the success of a systemic application against pancreatic cancer should encourage the use of gene therapy against various intractable diseases. It is of the utmost importance that a gene therapy possesses versatility in treating diseases; that is, once an appropriate delivery platform has been established, it can treat myriad diseases simply by using the appropriate combination of therapeutic genes and targeting ligands. Thus, we believe that establishing a systemic delivery system may have a tremendous impact on the future of medicine's ability to enrich human welfare. Such a smart delivery device could be prepared by integrating a variety of versatile molecular technologies to build the structures and functionalities necessary to achieve maximum performance and therapeutic results.

ACKNOWLEDGEMENTS

This work was financially supported by the Precursory Research for Embryonic Science and Technology (PRESTO) from the Japan Science and Technology Corporation (JST) and by the Japan Society for the Promotion of Science (JSPS) through its Funding Program for World-Leading Innovative R&D on Science and Technology (FIRST Program), Grant-in-Aid for Specially Promoted Research, and Core to Core Program for Advanced Research Networks. The author expresses special thanks to Professor Kazunori Kataoka from the University of Tokyo for his valuable direction in conducting this research. The TEM and Cryo-TEM observations were conducted in the Research Hub for Advanced Nano Characterization, the University of Tokyo, supported by the Ministry of Education, Culture, Sports, Science and Technology (MEXT) of Japan.

1 Ringsdorf, H. Structure and properties of pharmacologically active polymers. *J. Polym. Sci. Sym.* **51,** 135–153 (1975).
2 Kabanov, A. V. Polymer genomics: an insight into pharmacology and toxicology of nanomedicines. *Adv. Drug Deliver. Rev.* **58,** 1597–1621 (2006).
3 Cabral, H., Nishiyama, N. & Kataoka, K. Supramolecular nanodevices: from design validation to theranostic nanomedicine. *Acc. Chem. Res.* **44,** 999–1008 (2011).
4 Hubbell, J. A. & Chilkoti, A. Nanomaterials for drug delivery. *Science* **337,** 303–305 (2012).
5 Kopecek, J. Polymer-drug conjugates: origins, progress to date and future directions. *Adv. Drug Deliver. Rev.* **65,** 49–59 (2013).
6 Mulligan, R. C. The basic science of gene-therapy. *Science* **260,** 926–932 (1993).
7 Kay, M. A. State-of-the-art gene-based therapies: the road ahead. *Nat. Rev. Genet.* **12,** 316–328 (2011).
8 Zhang, Y., Satterlee, A. & Huang, L. *In vivo* gene delivery by nonviral vectors: overcoming hurdles? *Mol. Ther.* **20,** 1298–1304 (2012).
9 Owens, D. E. & Peppas, N. A. Opsonization, biodistribution, and pharmacokinetics of polymeric nanoparticles. *Int. J. Pharm.* **307,** 93–102 (2006).
10 Katayose, S. & Kataoka, K. Water-soluble polyion complex associates of DNA and poly(ethylene glycol)-poly(L-lysine) block copolymer. *Bioconjugate Chem.* **8,** 702–707 (1997).
11 Itaka, K., Ohba, S., Miyata, K., Kawaguchi, H., Nakamura, K., Takato, T., Chung, U. I. & Kataoka, K. Bone regeneration by regulated *in vivo* gene transfer using biocompatible polyplex nanomicelles. *Mol. Ther.* **15,** 1655–1662 (2007).
12 Itaka, K., Osada, K., Morii, K., Kim, P., Yun, S. H. & Kataoka, K. Polyplex nanomicelle promotes hydrodynamic gene introduction to skeletal muscle. *J. Control Release* **143,** 112–119 (2010).
13 Harada-Shiba, M., Yamauchi, K., Harada, A., Takamisawa, I., Shimokado, K. & Kataoka, K. Polyion complex micelles as vectors in gene therapy - pharmacokinetics and *in vivo* gene transfer. *Gene Therapy* **9,** 407–414 (2002).
14 Kanayama, N., Fukushima, S., Nishiyama, N., Itaka, K., Jang, W. D., Miyata, K., Yamasaki, Y., Chung, U. I. & Kataoka, K. A PEG-based biocompatible block catiomer with high buffering capacity for the construction of polyplex micelles showing efficient gene transfer toward primary cells. *Chemmedchem* **1,** 439–444 (2006).
15 Uchida, H., Miyata, K., Oba, M., Ishii, T., Suma, T., Itaka, K., Nishiyama, N. & Kataoka, K. Odd-even effect of repeating aminoethylene units in the side chain of n-substituted polyaspartamides on gene transfection profiles. *J. Am. Chem. Soc.* **133,** 15524–15532 (2011).
16 Miyata, K., Oba, M., Nakanishi, M., Fukushima, S., Yamasaki, Y., Koyama, H., Nishiyama, N. & Kataoka, K. Polyplexes from poly(aspartamide) bearing 1,2-diaminoethane side chains induce pH-selective, endosomal membrane destabilization with amplified transfection and negligible cytotoxicity. *J. Am. Chem. Soc.* **130,** 16287–16294 (2008).
17 Itaka, K., Ishii, T., Hasegawa, Y. & Kataoka, K. Biodegradable polyamino acid-based polycations as safe and effective gene carrier minimizing cumulative toxicity. *Biomaterials* **31,** 3707–3714 (2010).
18 Pack, D. W., Hoffman, A. S., Pun, S. & Stayton, P. S. Design and development of polymers for gene delivery. *Nat. Rev. Drug Discov.* **4,** 581–593 (2005).
19 Maeda, H., Nakamura, H. & Fang, J. The EPR effect for macromolecular drug delivery to solid tumors: improvement of tumor uptake, lowering of systemic toxicity, and distinct tumor imaging *in vivo*. *Adv. Drug Deliver. Rev.* **65,** 71–79 (2013).
20 Eisenberg, H. DNA flexing, folding, and function. *Account. Chem. Res.* **20,** 276–282 (1987).
21 Osada, K., Oshima, H., Kobayashi, D., Doi, M., Enoki, M., Yamasaki, Y. & Kataoka, K. Quantized folding of plasmid DNA condensed with block catiomer into characteristic rod structures promoting transgene efficacy. *J. Am. Chem. Soc.* **132,** 12343–12348 (2010).
22 Osada, K., Yamasaki, Y., Katayose, S. & Kataoka, K. A synthetic block copolymer regulates S1 nuclease fragmentation of supercoiled plasmid DNA. *Angew. Chem. Int. Edit.* **44,** 3544–3548 (2005).
23 Tinland, B., Pluen, A., Sturm, J. & Weill, G. Persistence length of single-stranded DNA. *Macromolecules* **30,** 5763–5765 (1997).
24 Smith, S. B., Cui, Y. J. & Bustamante, C. Overstretching B-DNA: the elastic response of individual double-stranded and single-stranded DNA molecules. *Science* **271,** 795–799 (1996).
25 Rackstraw, B. J., Martin, A. L., Stolnik, S., Roberts, C. J., Garnett, M. C., Davies, M. C. & Tendler, S. J. B. Microscopic investigations into PEG-cationic polymer-induced DNA condensation. *Langmuir* **17,** 3185–3193 (2001).
26 Jiang, X., Qu, W., Pan, D., Ren, Y., Williford, J. M., Cui, H., Luijten, E. & Mao, H. Q. Plasmid-templated shape control of condensed DNA-block copolymer nanoparticles. *Adv. Mater.* **25,** 227–232 (2013).
27 Ruff, Y., Moyer, T., Newcomb, C. J., Demeler, B. & Stupp, S. I. Precision templating with DNA of a virus-like particle with peptide nanostructures. *J. Am. Chem. Soc.* **135,** 6211–6219 (2013).
28 Osada, K., Shiotani, T., Tockary, T. A., Kobayashi, D., Oshima, H., Ikeda, S., Christie, R. J., Itaka, K. & Kataoka, K. Enhanced gene expression promoted by the quantized folding of pDNA within polyplex micelles. *Biomaterials* **33,** 325–332 (2012).
29 Oba, M., Miyata, K., Osada, K., Christie, R. J., Sanjoh, M., Li, W. D., Fukushima, S., Ishii, T., Kano, M. R., Nishiyama, N., Koyama, H. & Kataoka, K. Polyplex micelles prepared from omega-cholesteryl PEG-polycation block copolymers for systemic gene delivery. *Biomaterials* **32,** 652–663 (2011).
30 Tockary, T. A., Osada, K., Chen, Q., Machitani, K., Dirisala, A., Uchida, S., Nomoto, T., Toh, K., Matsumoto, Y., Itaka, K., Nitta, K., Nagayama, K. & Kataoka, K. Tethered PEG crowdedness determining shape and blood circulation profile of polyplex micelle gene carriers. *Macromolecules* **46,** 6585–6592 (2013).
31 Lee, M. & Kim, S. W. Polyethylene glycol-conjugated copolymers for plasmid DNA delivery. *Pharm. Res.* **22,** 1–10 (2005).
32 Li, S. D. & Huang, L. Stealth nanoparticles: high density but Sheddable PEG is a key for tumor targeting. *J. Control. Release* **145,** 178–181 (2010).
33 Jokerst, J. V., Lobovkina, T., Zare, R. N. & Gambhir, S. S. Nanoparticle PEGylation for imaging and therapy. *Nanomedicine* **6,** 715–728 (2011).
34 Kenausis, G. L., Voros, J., Elbert, D. L., Huang, N. P., Hofer, R., Ruiz-Taylor, L., Textor, M., Hubbell, J. A. & Spencer, N. D. Poly(L-lysine)-g-poly(ethylene glycol) layers on metal oxide surfaces: attachment mechanism and effects of polymer architecture on resistance to protein adsorption. *J. Phys. Chem. B* **104,** 3298–3309 (2000).
35 Meister, A. & Anderson, M. E. Glutathione. *Annu. Rev. Biochem.* **52,** 711–760 (1983).
36 Miyata, K., Kakizawa, Y., Nishiyama, N., Harada, A., Yamasaki, Y., Koyama, H. & Kataoka, K. Block catiomer polyplexes with regulated densities of charge and disulfide cross-linking directed to enhance gene expression. *J. Am. Chem. Soc.* **126,** 2355–2361 (2004).
37 Oba, M., Aoyagi, K., Miyata, K., Matsumoto, Y., Itaka, K., Nishiyama, N., Yarnasaki, Y., Koyama, H. & Kataoka, K. Polyplex micelles with cyclic RGD peptide ligands and disulfide cross-links directing to the enhanced transfection via controlled intracellular trafficking. *Mol. Pharmaceut.* **5,** 1080–1092 (2008).
38 Ge, Z., Chen, Q., Osada, K., Liu, X., Tockary, T. A., Uchida, S., Dirisala, A., Ishii, T., Nomoto, T., Toh, K., Matsumoto, Y., Oba, M., Kano, M. R., Itaka, K. & Kataoka, K. Targeted gene delivery by polyplex micelles with crowded PEG palisade and cRGD moiety for systemic treatment of pancreatic tumors. *Biomaterials* **35,** 3416–3426 (2014).
39 Walker, G. F., Fella, C., Pelisek, J., Fahrmeir, J., Boeckle, S., Ogris, M. & Wagner, E. Toward synthetic viruses: endosomal ph-triggered deshielding of targeted polyplexes greatly enhances gene transfer *in vitro* and *in vivo*. *Mol. Ther.* **11,** 418–425 (2005).
40 Meyer, M. & Wagner, E. pH-Responsive shielding of non-viral gene vectors. *Exp. Opin. Drug deliv.* **3,** 563–571 (2006).
41 Takae, S., Miyata, K., Oba, M., Ishii, T., Nishiyama, N., Itaka, K., Yamasaki, Y., Koyama, H. & Kataoka, K. PEG-Detachable polyplex micelles based on disulfide-linked block catiomers as bioresponsive nonviral gene vectors. *J. Am. Chem. Soc.* **130,** 6001–6009 (2008).
42 Hatakeyama, H., Akita, H., Ito, E., Hayashi, Y., Oishi, M., Nagasaki, Y., Danev, R., Nagayama, K., Kaji, N., Kikuchi, H., Baba, Y. & Harashima, H. Systemic delivery of siRNA to tumors using a lipid nanoparticle containing a tumor-specific cleavable PEG-lipid. *Biomaterials* **32,** 4306–4316 (2011).
43 Manjappa, A. S., Chaudhari, K. R., Venkataraju, M. P., Dantuluri, P., Nanda, B., Sidda, C., Sawant, K. K. & Murthy, R. S. R. Antibody derivatization and conjugation strategies: application in preparation of stealth immunoliposome to target chemotherapeutics to tumor. *J. Control Release* **150,** 2–22 (2011).

44 Torchilin, V. P. Tat peptide-mediated intracellular delivery of pharmaceutical nanocarriers. *Adv. Drug Deliver. Rev.* **60,** 548–558 (2008).
45 Sawant, R. & Torchilin, V. Intracellular transduction using cell-penetrating peptides. *Mol. Biosyst.* **6,** 628–640 (2010).
46 Bolhassani, A. Potential efficacy of cell-penetrating peptides for nucleic acid and drug delivery in cancer. *Bba-Rev. Cancer* **1816,** 232–246 (2011).
47 Wagner, E., Curiel, D. & Cotten, M. Delivery of drugs, proteins and genes into cells using transferrin as a ligand for receptor-mediated endocytosis. *Adv. Drug Deliver. Rev.* **14,** 113–135 (1994).
48 Jenkins, R. G., Herrick, S. E., Meng, Q. H., Kinnon, C., Laurent, G. J., McAnulty, R. J. & Hart, S. L. An integrin-targeted non-viral vector for pulmonary gene therapy. *Gene Ther* **7,** 393–400 (2000).
49 Kircheis, R., Wightman, L., Kursa, M., Ostermann, E. & Wagner, E. Tumor-targeted gene delivery: an attractive strategy to use highly active effector molecules in cancer treatment. *Gene Ther.* **9,** 731–735 (2002).
50 Chen, Y. C., Wu, J. Z. J. & Huang, L. Nanoparticles targeted with NGR motif deliver c-myc siRNA and doxorubicin for anticancer therapy. *Mol. Ther.* **18,** 828–834 (2010).
51 Garanger, E., Boturyn, D., Jin, Z., Dumy, P., Favrot, M. C. & Coll, J. L. New multifunctional molecular conjugate vector for targeting, imaging, and therapy of tumors. *Mol. Ther.* **12,** 1168–1175 (2005).
52 Mickler, F. M., Vachutinsky, Y., Oba, M., Miyata, K., Nishiyama, N., Kataoka, K., Brauchle, C. & Ruthardt, N. Effect of integrin targeting and peg shielding on polyplex micelle internalization studied by live-cell imaging. *J. Control. Release* **156,** 364–373 (2011).
53 Mancuso, A., Calabro, F. & Sternberg, C. N. Current therapies and advances in the treatment of pancreatic cancer. *Crit. Rev. Oncol. Hemat.* **58,** 231–241 (2006).
54 Cabral, H., Matsumoto, Y., Mizuno, K., Chen, Q., Murakami, M., Kimura, M., Terada, Y., Kano, M. R., Miyazono, K., Uesaka, M., Nishiyama, N. & Kataoka, K. Accumulation of sub-100 nm polymeric micelles in poorly permeable tumours depends on size. *Nat. Nanotechnol.* **6,** 815–823 (2011).
55 Folkman, J., Bach, M., Rowe, J. W., Davidoff, F., Lambert, P., Hirsch, C., Goldberg, A., Hiatt, H. H., Glass, J. & Henshaw, E. Tumor angiogenesis - therapeutic implications. *New Engl. J. Med.* **285,** 1182–1186 (1971).
56 Carmeliet, P. & Jain, R. K. Angiogenesis in cancer and other diseases. *Nature* **407,** 249–257 (2000).
57 Kong, H. L., Hecht, D., Song, W., Kovesdi, I., Hackett, N. R., Yayon, A. & Crystal, R. G. Regional suppression of tumor growth by *in vivo* transfer of a cDNA encoding a secreted form of the extracellular domain of the Flt-1 vascular endothelial growth factor receptor. *Hum. Gene Ther.* **9,** 823–833 (1998).
58 Oba, M., Vachutinsky, Y., Miyata, K., Kano, M. R., Ikeda, S., Nishiyama, N., Itaka, K., Miyazono, K., Koyama, H. & Kataoka, K. Antiangiogenic gene therapy of solid tumor by systemic injection of polyplex micelles loading plasmid DNA encoding soluble Flt-1. *Mol. Pharm.* **7,** 501–509 (2010).
59 Cabral, H., Nishiyama, N. & Kataoka, K. Optimization of (1,2-diamino-cyclohexane)-platinum(II)-loaded polymeric micelles directed to improved tumor targeting and enhanced antitumor activity. *J. Control. Release* **121,** 146–155 (2007).
60 Osada, K., Cabral, H., Mochida, Y., Lee, S., Nagata, K., Matsuura, T., Yamamoto, M., Anraku, Y., Kishimura, A., Nishiyama, N. & Kataoka, K. Bioactive polymeric metallosomes self-assembled through block copolymer-metal complexation. *J. Am. Chem. Soc.* **134,** 13172–13175 (2012).
61 Kanwar, Y. S. & Farquhar, M. G. Presence of heparan sulfate in the glomerular basement membrane. *Proc. Natl Acad. Sci. USA* **76,** 1303–1307 (1979).
62 Zuckerman, J. E., Choi, C. H., Han, H. & Davis, M. E. Polycation-siRNA nanoparticles can disassemble at the kidney glomerular basement membrane. *Proc. Natl Acad. Sci. USA* **109,** 3137–3142 (2012).